

# Applicability of wavelet algorithm for geophysical viscoelastic flow

Oleg V. Vasilyev,<sup>1</sup> David A. Yuen,<sup>2</sup> and Yuri Yu. Podladchikov<sup>3</sup>

**Abstract.** This paper introduces a newly developed wavelet technique for modeling of geophysical flow processes in multiple dimensions. The method utilizes the idea of collocation with the multilevel wavelet approximation. The multilevel structure of the algorithm facilitates the computational adaptation of the grid refinement in regions where sharp variations occur. We have tested this algorithm for viscoelastic flows with viscosity contrasts up to  $10^{12}$ . We have confirmed the findings of stress amplification in the thin highly viscous layer. The new method allows us to conduct the calculations for thin layers and high viscosity contrasts, close enough for realistic mantle-lithospheric interaction. Our results demonstrate the potential usefulness of the wavelet technique in large-scale numerical simulations in the geosciences.

## Introduction

Wavelet theory has now been around for nearly a decade. However, most of the applications of wavelets in geosciences have been focussed on analyzing data [Kumar and Fofoula-Georgiou, 1993; Li and Loehle, 1995] and there remains a large gap in applying wavelets for solving the difficult partial differential equations (PDE) in geophysics. The objective of this paper is to communicate the need for looking at wavelets as a potential, viable tool in large-scale numerical modeling of geophysical flow problems and to bridge this communication gap by providing a short description of wavelet based numerical algorithm and its advantages over conventional numerical methods.

If the solution of a geophysical flow problem has regular features, any of the conventional numerical techniques can be applied. However, in many problems in geophysics there exists a multiplicity of very different spatial and temporal scales in the solution, as in strongly time-dependent non-Newtonian convection [Malevsky *et al.*, 1992; Larsen *et al.*, 1995], in faulting problems [Ben-Zion and Rice, 1993; Poliakov *et al.*, 1994], or in rising diapirs with sharp viscosity gradients [Weinberg and Podladchikov, 1995]. This particular attribute of multiple spatial scales requires an efficient adaptive multi-scale numerical algorithm. In this respect wavelet based numerical algorithms are ideally suited for geophysical problems, since they provide a simple, efficient and automatic way to adapt computational refinements to

local demands of the solution. Far fewer grid points are needed for wavelets than for conventional non-adaptive finite-difference or finite-element techniques.

The applicability of wavelet based numerical algorithms to geophysical problems is illustrated by the solution of the viscoelastic model problem, using a dynamically adaptive wavelet collocation method [Vasilyev and Paolucci, 1997]. The problem is similar to the one described in [Poliakov *et al.*, 1993]. A very thin upper boundary layer, the lithosphere, which is quasi-elastic, interacts with a highly variable viscous mantle.

## Mathematical Model

Consider a plane-strain viscoelastic flow with a strongly variable viscosity driven by density inhomogeneities in a vertical rectangular domain. Superscript “\*” denotes dimensional quantities. The characteristic scales are the size of the domain  $L^*$ , the reference dynamic viscosity  $\mu^*$ , the shear elastic modulus  $G^*$ , and gravity force per unit volume  $\rho^*g^*$ , where  $\rho^*$  is the characteristic scale for the density deviations and  $g^*$  is the gravity acceleration. There is also an extra parameter “inertial density”  $\rho_i^*$ , which may not equal to the  $\rho^*$  [Poliakov *et al.*, 1993]. The three independent scales used in dimensional analyses are  $L^*$ ,  $\mu^*$  and  $\rho^*g^*$ , which makes the stress, time and velocity scales to be  $\rho^*g^*L^*$ ,  $\mu^*/(\rho^*g^*L^*)$  and  $(\rho^*g^*(L^*)^2)/\mu^*$  respectively. We denote the non-dimensional pressure, three in-plane deviatoric components of stress tensor, and velocity components in  $x_1$  and  $x_2$  directions by  $p$ ,  $\tau_{11}$ ,  $\tau_{22}$ ,  $\tau_{12}$ ,  $V_1$ , and  $V_2$  respectively. The viscoelastic equations described in [Poliakov *et al.*, 1993] are given by

$$\begin{aligned} \frac{\partial V_i}{\partial t} &= \frac{1}{Re} \left[ -\frac{\partial p}{\partial x_i} + \frac{\partial \tau_{ij}}{\partial x_j} + \rho e_{gi} \right], \\ \frac{\partial p}{\partial t} &= -\frac{K}{De} \frac{\partial V_i}{\partial x_i}, \\ \frac{\partial \tau_{ij}}{\partial t} &= \frac{1}{De} \left[ -\frac{\tau_{ij}}{2\mu} + \frac{1}{2} \left( \frac{\partial V_i}{\partial x_j} + \frac{\partial V_j}{\partial x_i} \right) - \frac{1}{3} \frac{\partial V_k}{\partial x_k} \delta_{ij} \right], \end{aligned} \quad (1)$$

where  $i, j, k = 1, 2$ , repeated indices imply the summation,  $\delta_{ij}$  is the Kronecker delta, and  $e_{gi} = (0, -1)$  is the unity vector along gravity. The independent dimensionless parameters appearing in the equations are

$$Re = \frac{\rho_i^* \rho^* g^* (L^*)^3}{(\mu^*)^2}, \quad De = \frac{\rho^* g^* L^*}{G^*}, \quad K = \frac{K^*}{G^*}, \quad (2)$$

where  $K^*$  is the bulk elastic modulus. These parameters represent the Reynolds and Deborah numbers, and the measure of the ratio of bulk and shear elastic moduli. Although equations (1) can be rescaled in such a way that some of the parameters are omitted, we have chosen this form for geophysical relevance. The density perturbation  $\rho$  is chosen to

<sup>1</sup>Center for Turbulence Research, Stanford, California.

<sup>2</sup>Minnesota Supercomputer Institute and Department of Geology and Geophysics, University of Minnesota, Minneapolis, Minnesota.

<sup>3</sup>Geologisches Institut, ETH-Zurich, Zurich, Switzerland.

be  $\rho(x_1, x_2) = 0.1x_2 \cos(\pi x_1)$ , which serves the purpose of driving the flow. The non-dimensional viscosity  $\mu$  is taken to be  $\mu(x_1, x_2) = (\mu_0 + (\mu_1 - \mu_0) f_1(x_2)) (1 - f_2(x_1, x_2)) + \mu_0 f_2(x_1, x_2)$ , where  $f_1(x_2) = \exp\left[-\frac{(x_2-1)^2}{\lambda^2}\right]$  and

$f_2(x_1, x_2) = \exp\left[-\frac{(x_1-x_{10})^2 + (x_2-x_{20})^2}{r_0^2}\right]$ . Constants  $\mu_0, \mu_1, \mu_2, \lambda, r_0$  and functions  $f_1$  and  $f_2$  are chosen in such a way that high viscosity region is concentrated near the top ( $f_1$ ), in addition, a low viscosity ‘‘spot’’ is placed in the neighborhood of  $(x_{10}, x_{20})$  ( $f_2$ ). The problem is solved for  $Re = 10^{-3}$ ,  $De = 10^{-2}$ ,  $K = 1$ ,  $\mu_0 = 1$ ,  $\mu_1 = 10^8$ , and  $(x_{10}, x_{20}) = (1, 0.5)$ . The parameter  $\mu_2$  is chosen to be either 1 or  $10^{-4}$ , depending on whether the low viscosity spot is present or not. We have used two sets of geometrical parameters  $\lambda$  and  $r_0$ . The first set is  $\lambda = 0.02$  and  $r_0 = 0.05$  and the second is  $\lambda = 0.005$  and  $r_0 = 0.025$ . The initial and boundary conditions are respectively given by

$$\begin{aligned} V_i(x_1, x_2, t)|_{t=0} &= p(x_1, x_2, t)|_{t=0} = \tau_{ij}(x_1, x_2, t)|_{t=0} = 0, \\ V_1(x_1, x_2, t)|_{x_1=0,1} &= V_2(x_1, x_2, t)|_{x_2=0,1} = 0, \\ \tau_{12}(x_1, x_2, t)|_{x_1=0,1} &= \tau_{21}(x_1, x_2, t)|_{x_2=0,1} = 0. \end{aligned}$$

## Computational Method

Here we briefly describe the numerical algorithm which we will use to solve the system of equations (1). For more details about the algorithm, we refer the reader to [Vasilyev, 1996] and [Vasilyev and Paolucci, 1997].

### Fast Wavelet Collocation Transform

Let us consider a function  $u(x_1, x_2)$  defined on a closed rectangular domain. We take

$$\psi_{k,l}^j(x_1, x_2) = \psi\left(\frac{x_1 - b_{1k}^j}{a_{1j}}, \frac{x_2 - b_{2l}^j}{a_{2j}}\right), \quad (3)$$

where  $\psi(x_1, x_2)$  is a two-dimensional wavelet (or scaling function),  $\psi_{k,l}^j(x_1, x_2)$  is a wavelet of  $j$  level of resolution with scales  $a_{1j}$  and  $a_{2j}$  and location  $(b_{1k}^j, b_{2l}^j)$ . It can be shown [Vasilyev and Paolucci, 1997] that  $u(x_1, x_2)$  can be approximated as

$$u^J(x_1, x_2) = \sum_{j=0}^J \sum_{(k,l)} c_{k,l}^j \psi_{k,l}^j(x_1, x_2), \quad (4)$$

where the approximation is composed of wavelets whose amplitudes satisfy the following criteria

$$|c_{k,l}^j| \geq \epsilon. \quad (5)$$

The distinctive feature of the wavelet approximation (4) is its multilevel nature. In other words, various scales present in the function are approximated by wavelets of different levels of resolution. Given the values of function at the collocation points, which are chosen to be wavelet locations, wavelet coefficients at all levels of resolution are found by using fast wavelet collocation transform (FWCT). Knowing  $c_{i,k}^j$  at all levels of resolution, the values of the derivatives of the approximate function at the collocation points can be found by using fast inverse wavelet collocation transform (FIWCT). Due to the compact support of the basic wavelet and the cardinal properties ( $\psi(i, k) = \delta_{i,0} \delta_{k,0}$ ) of wavelets in

this algorithm, the total computational cost of both FWCT and FIWCT is  $O((J+1)M_W^2 \mathcal{N})$  operations, where  $\mathcal{N}$  is the total number of collocation points and  $M_W$  is a parameter characterizing the wavelet support.

### Dynamically Adaptive Numerical Algorithm

Following the classical collocation approach for evaluating PDE’s, we obtain a system of ordinary differential equations. Derivatives of the functions in the equations are formed as described above.

In order for the algorithm to resolve all the structures, the basis of active wavelets and, consequently, the computational grid should be adapted dynamically in time to reflect local changes in the solution. This changing of the computational grid is based on the analysis of wavelet coefficients. The contribution of a wavelet into the approximation is considerable if and only if the nearby structures of the solution have comparable size with the wavelet scale. Thus, we may drop the large number of fine scale wavelets with small coefficients in the regions where the solution is smooth. This property of the multilevel wavelet approximation allows local grid refinement up to an arbitrary small scale without a drastic increase of the number of grid points.

To ensure the accuracy, the basis should also consist of wavelets whose coefficients can possibly become significant during the period of time in between grid adaptation. Thus, at any instant of time, the basis should not only include wavelets satisfying criterion (5), but also the surrounding wavelets.

Let us denote by  $\mathcal{G}_{\geq}^t$  the irregular grid of wavelet collocation points which are retained to approximate the solution at time  $t$ . The numerical algorithm consists of three steps:

1. From the values of the solution  $u_{i,k}^J(t)$  we compute the values of wavelet coefficients using FWCT. For a given threshold  $\epsilon$  we adjust  $\mathcal{G}_{\geq}^{t+\Delta t}$ .
2. If there are no changes between  $\mathcal{G}_{\geq}^t$  and  $\mathcal{G}_{\geq}^{t+\Delta t}$ , we go directly to step 3. Otherwise, we compute the values of the solution on  $\mathcal{G}_{\geq}^{t+\Delta t}$ , which are not included in  $\mathcal{G}_{\geq}^t$ .
3. Integrate the resulting system of ordinary differential equations to obtain new values  $u_{i,k}^J(t + \Delta t)$  and go back to step 1.

The basic hypothesis motivating the algorithm is that during a time interval  $\Delta t$ , the domain of wavelets with significant coefficients does not move abruptly in the phase space of wavelet coefficients. The irregular grid of wavelet collocation points is dynamically adapted in time and follows the local structures that appear in the solution. By omitting wavelets with coefficients below a threshold parameter  $\epsilon$ , we automatically control the error of approximation. Thus wavelet collocation method has an *active control* of the accuracy of the solution. The smaller  $\epsilon$  is chosen the smaller the error of the solution is. Typically the value of  $\epsilon$  varies between  $10^{-2}$  and  $10^{-4}$ .

## Results and Discussion

The results have been obtained by using the dynamically adaptive multilevel collocation method. The correlation function of Daubechies scaling function of order five [Beylkin and Saito, 1993] was employed with the threshold parameter  $\epsilon = 10^{-2}$ , which means that the local relative

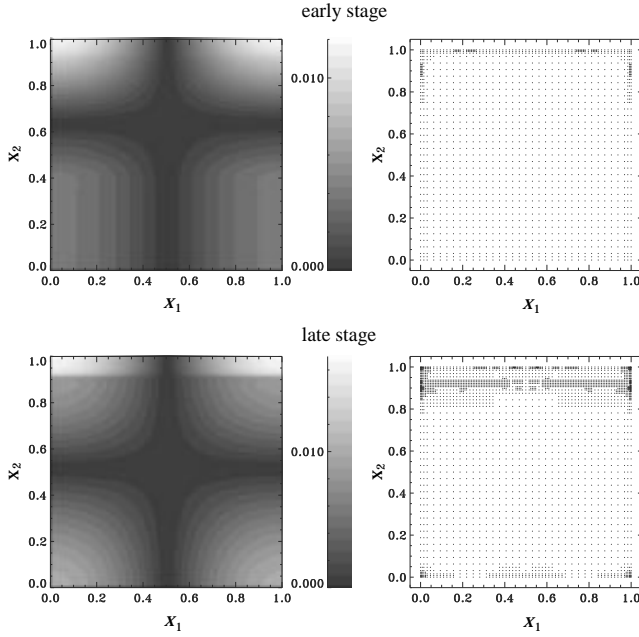


**Figure 1.** Absolute value of the  $\tau_{11}$  component of stress tensor and the associated computational grid for  $\lambda = 0.02$  at two different times.

error is everywhere less than  $10^{-2}$ . The adaptation of the computational grid is based on the analysis of coefficients associated with all six dependent variables of equations (1). The irregular grid  $\mathcal{G}_z^c$  of wavelet collocation points is constructed as a union of irregular grids corresponding to each dependent variable.

The solution for the  $\tau_{11}$  component of stress tensor and corresponding to the computational grid for the case of  $\lambda = 0.02$  is illustrated in Figure 1 for two different times. The high stress region is observed at the top 8% of the domain. With the decrease of  $\lambda$  and consequently the high viscosity region, the thickness of the high stress is decreased accordingly. This phenomena, which we call *stress-focusing effect*, is illustrated in Figure 2 corresponding to the case of  $\lambda = 0.005$  and 2% high stress region. The zoomed-in high viscosity region and corresponding computational grid is also shown in Figure 2. It can be seen that the computational grid is dense only in the neighborhood of small scale structures, such as high stress concentration region.

The capability of the numerical algorithm to resolve localized two dimensional structures such as low viscosity spot is illustrated in Figure 3. The zoomed-in low viscosity spot region and corresponding computational grid are shown there as well. The effect of low viscosity spot region can be seen from comparison of computational grids of Figure 2 and Figure 3. We see the dense computational grid surrounding the low viscosity spot. From comparing the solution and the computational grid, we can observe that the computational grid is very fine only in the regions where small scale features or large gradients are present. The total number of grid points at any instant of time did not exceed  $10^4$  for all cases presented here, while if one repeats the same calculation on a non-adaptive grid using conventional numerical algorithms, it would require more than  $10^6$  regularly spaced grid points.

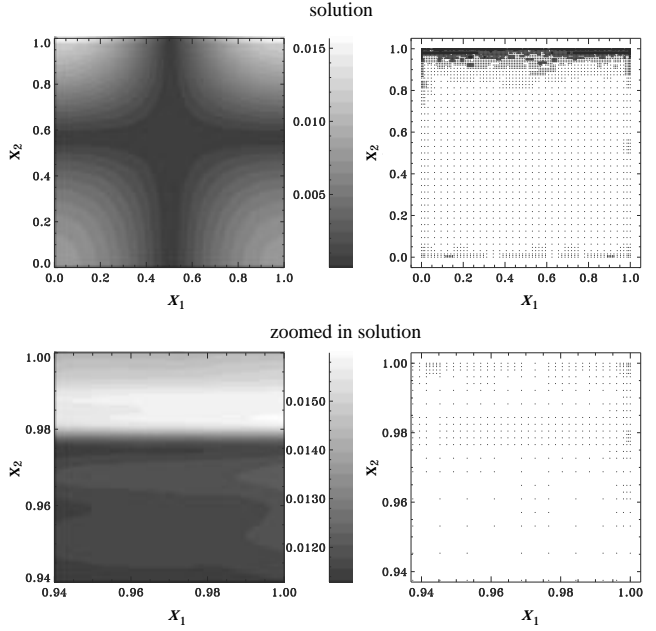


**Figure 2.** Solution and zoomed-in view of the high viscosity region for the absolute value of the  $\tau_{11}$  component of stress tensor and the associated computational grid for  $\lambda = 0.005$ ,  $\mu_2 = 1$ .

We have applied a new adaptive wavelet based method to solving PDEs arising in a geophysical context. The algorithm has been employed for a viscoelastic flow having strong variations in viscosity. We have verified the previous findings of stress amplification in the thin high viscous layer [Kuznir and Bott, 1977, Poliakov et al., 1993, Podlad-

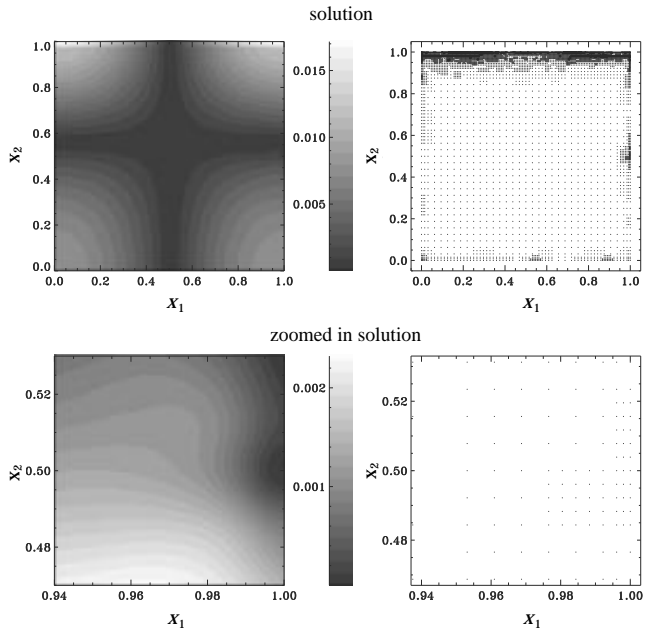


**Figure 3.** Solution and zoomed-in view of the low viscosity spot region for the absolute value of the  $\tau_{11}$  component of stress tensor and the associated computational grid for  $\lambda = 0.005$ ,  $\mu_2 = 10^{-4}$ .

*chikov et al.*, 1993]. The new method allows us to conduct the calculations close enough for realistic lithosphere-mantle interaction. This highly adaptive wavelet based method allows us to resolve much thinner lithosphere and higher viscosity contrasts with considerable reduction in the number of unknowns as compared to conventional finite-difference method [Poliakov *et al.*, 1993]. High-resolution computations afforded by adaptive wavelet based method are needed to follow the evolution of the stress-focusing process in a plastic lithosphere, which results in localization in the strain field [Tapponier and Molnar, 1976]. Similar computational problems arise in modeling of faulting of brittle overburden over viscous substratum at smaller (few km) scale [Poliakov *et al.*, 1995].

**Acknowledgments.** This research has been supported by Cray Research Inc and the geophysics program of National Science Foundation.

## References

- Ben-Zion, Y., and J. R. Rice, Earthquake failure sequences along a cellular fault zone in a three-dimensional elastic solid containing asperity and non-asperity regions, *J. Geophys. Res.*, **98**, 14109-14131, 1993.
- Beylkin, G., and N. Saito, Wavelets, their autocorrelation function and multidimensional representation of signals, in *Proceedings of SPIE - The International Society of Optical Engineering*, Vol. *LB26*, Int. Soc. for Optical Engineering, Bellingham, 1993.
- Kumar, P., and E. Foufoula-Georgiou, A multicomponent decomposition of spatial rainfall fields: 1. Segregation of large and small scale features using wavelet transforms, *Water Resources Research*, **29**, 2515-2532, 1993.
- Kuznir, N. J., and M. H. P. Bott, Stress concentration in the upper lithosphere caused by underlying viscoelastic creep, *Tectonophysics*, **43**, 247-256, 1977.
- Larsen, T. B., D. A. Yuen, and A. V. Malevsky, Dynamical consequences on fast subducting slabs from a self-regulating mechanism due to viscous heating in variable viscosity convection, *Geophys. Res. Lett.*, **22**, 1277-1280, 1995.
- Li, B. L., and C. Loehle, Wavelet analysis of multiscale permeabilities in the subsurface, *Geophys. Res. Lett.*, **22**, 3123-3126, 1995.
- Malevsky, A. V., D. A. Yuen, and L. M. Weyer, Viscosity and thermal fields associated with strongly chaotic non-Newtonian thermal convection, *Geophys. Res. Lett.*, **19**, 27-30, 1992.
- Poliakov, A. N. B., P. A. Cundall, Yu. Yu. Podladchikov, and V. A. Lyakhovskiy, An explicit inertial method for the simulation of visco-elastic flow, an evaluation of elastic effects on diapiric flow in two- and three-layer models, in *Flow and Creep in the Solar System: Observations, Modelling and Theory*, edited by D.B. Stone and S.K. Runcorn, pp 175-196, Kluwer Academic Publishers, Dordrecht, Holland, 1993.
- Poliakov A.N., H. J. Herrmann, Yu. Yu. Podladchikov, and S. Roux, Fractal plastic shear bands, *Fractals*, **2**, 567-581, 1994.
- Poliakov A., Yu. Yu. Podladchikov, E. Dawson E., and C. Talbot, Salt diapirism with simultaneous brittle faulting and viscous flow, in *Salt Tectonics, Geological Society Special Publication No 100*, edited by G.I. Alsop, D.J. Blundell and I. Davison, 1995.
- Podladchikov, Yu. Yu., A. Lenardic, D. A. Yuen, and F. Quarenii, Dynamical consequences of stress focussing for different rheologies: Earth and Venus perspectives, *EOS Trans. AGU*, fall meeting suppl., **74**, p598, 1993.
- Tapponier, P., and P. Molnar, Slip line field theory and large scale continental tectonics, *Nature*, **264**, 319-324, 1976.
- Vasilyev, O. V., Multilevel Wavelet Collocation Methods for Solving Partial Differential Equations, Ph.D. Thesis, University of Notre Dame, May 1996.
- Vasilyev, O. V., and S. Paolucci, A fast adaptive wavelet collocation algorithm for multi-dimensional PDEs. *To appear in J. Comp. Phys.*, 1997.
- Weinberg, R. F., and Yu. Yu. Podladchikov, The rise of solid-state diapirs, *J. Structural Geology*, **17**, 1183-1195, 1995.

---

Oleg V. Vasilyev, Center for Turbulence Research, Stanford University, Bldg 500, Stanford, CA 94305-3030.

David A. Yuen, Minnesota Supercomputer Institute and Department of Geology and Geophysics, University of Minnesota, Minneapolis, MN 55415-1227.

Yuri Yu. Podladchikov, Geologisches Institut, ETH-Zurich, Sonneggstr. 5, CH 8092, Zurich, Switzerland

(Received June 24, 1997; revised October 20, 1997; accepted October 23, 1997.)